

Broadband and Wavelength-Dependent Chalcogenide Optical Fiber Couplers

Farzan Tavakoli, Alexandre Rekik, and Martin Rochette, *Senior Member, IEEE*

Abstract—We present optical fiber couplers made of As₂Se₃ glass. Broadband and wavelength-dependent couplers are fabricated from fibers of engineered core/cladding diameter ratios. Coupling ratios at the through-cross ports ranging from 50%–50% down to 1%–99% are achieved. The transparency of As₂Se₃ glass over the spectral range of 1.5–12.0 μm makes it a material of prime interest for the fabrication of mid-infrared couplers.

Index Terms—Chalcogenide glasses, mid-infrared optical fiber coupler, broadband and wavelength-dependent couplers, stretching setup, adiabaticity criteria, power vs. extension graph.

I. INTRODUCTION

OPTICAL fiber couplers are essential building blocks of any optical fiber device or system. They are commonly classified in two separate categories that are broadband and wavelength-dependent, depending on the target application. The broadband coupler is often used as a power-divider or tap-coupler, whereas the wavelength-dependent coupler is often used in wavelength-division multiplexing applications, or also serves to combine a signal and a pump in a rare-earth-doped fiber. The currently widespread silica fiber couplers are unfortunately impaired by intrinsic absorption when targeting applications at wavelengths beyond 2.0 μm . As an ideal material for the fabrication of mid-infrared optical components, chalcogenide (ChG) glasses such as As₂Se₃ are of great interest owing to their broadband transparency in the spectral range from 1.5 μm up to 12.0 μm [1]. In a previous report, a multimode fused coupler was made of ChG fibers using an As₄₀S₅₈Se₂ core with a diameter of 135 μm and an As₄₀S₆₀ cladding with a diameter of 200 μm [2], [3]. The coupler sustained highly multimode operation at a wavelength of 2.7 μm with a coupling ratio of 67%–33% at the through-cross ports, respectively. Thus, a maximum of one third of the input power could be transferred from the input port to the cross-port. Moreover, the wavelength dependence of the coupler was not investigated. In a recent report, fused ZBLAN fiber couplers were successfully fabricated and tested [4]; however, ZBLAN glass provides transparency up to 7.0 μm

representing a fraction of the spectrum available with ChG glasses (1.5 μm –12.0 μm).

To the best of our knowledge, no fiber coupler with quasi-single mode or wavelength-selective operation has been reported yet which provides arbitrary coupling ratios [5].

In this letter, we present the successful fabrication of two As₂Se₃ couplers that are compatible with the mid-infrared: one that is broadband and one that is wavelength-dependent. The broadband coupler is quasi single-mode and provides a coupling ratio ~ 3 dB spreading from 1.5 μm up to 2.0 μm . The wavelength-dependent coupler has a period of ~ 6.25 THz with an extinction ratio > 15 dB between the through and cross ports at transmission maxima. The heat-brush technique used in the fabrication process leads to arbitrary coupling ratios ranging from 1%–99%, and passing by 50%–50% at the through-cross ports, respectively, with little or large wavelength-dependence.

II. COUPLER THEORY

The analysis and design of optical couplers are commonly performed using coupled-mode theory (CMT) [6]. The theory is based on the perturbation of the fundamental mode propagating in each fiber rather than treating the waveguide structure as a whole and propagating the eigenmodes (or supermodes) of the entire cross-sectional geometry. Using CMT for the general case of an asymmetric coupler leads to:

$$\frac{P_X(L)}{P_0} = \frac{|\kappa|^2}{\beta_c^2} \sin^2(\kappa L) \quad (1a)$$

$$\kappa = \frac{K_0 \left(\frac{WD}{r_0} \right) U^2}{k_0 n_1 (r_0 V K_1(W))^2} \quad (1b)$$

$$\beta_c^2 = |\kappa|^2 + \delta^2 \quad (1c)$$

where P_X is the cross-port output power, P_0 is the power in the input port, κ is the coupling coefficient for a symmetric fiber coupler, β_c is the corrected coupling coefficient for an asymmetric coupler, δ is the phase mismatch parameter, k_0 is the wavenumber, r_0 is the radius of each fiber, D is the separation between the cores, $V = k_0 r_0 N A$ is the V-number, $W = r_0 (\beta^2 - n_2^2 k_0^2)^{1/2}$, $U = r_0 (n_1^2 k_0^2 - \beta^2)^{1/2}$, β is the propagation constant, n_1 and n_2 are the core and cladding refractive indices, K_0 and K_1 are 0th and 1st order Bessel functions of the second kind and L is the fusion length of the coupler. δ has a significant importance since it is a measure of coupler symmetry showing to what degree the two fibers constituting the coupler are identical.

Manuscript received December 21, 2016; revised March 3, 2017; accepted March 10, 2017. Date of publication March 15, 2017; date of current version April 13, 2017. This work was supported in part by Coractive High-Tech and in part by the Natural Sciences and Engineering Research Council of Canada. (Corresponding author: Farzan Tavakoli.)

The authors are with the Department of Electrical and Computer Engineering, McGill University, Montréal, QC H3A 0E9, Canada (e-mail: farzan.tavakoli@mail.mcgill.ca; martin.rochette@mcgill.ca).

Color versions of one or more of the figures in this letter are available online at <http://ieeexplore.ieee.org>.

Digital Object Identifier 10.1109/LPT.2017.2682821

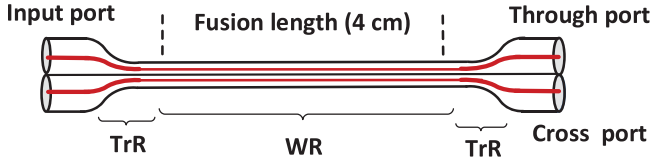


Fig. 1. ChG coupler geometry. TrR, transition region; WR, waist region.

The specific case for which the coupler is truly-symmetric requires that $\delta = 0$ and thus:

$$P_X = P_0 \sin^2(\kappa(\lambda)L) \quad (2)$$

For a fixed κ , the power transferred to the cross-port is a cyclic function of the propagation distance. Coupling length (L_c) is defined as the minimum length required to get a complete power transfer from the input port to the cross-port:

$$L_c = \frac{\pi}{2\kappa} \quad (3)$$

As equation (2) suggests, wavelength periodicity of the coupler is proportional to $|d\kappa/d\lambda|$. From equation (1-b), κ is a transcendental function of λ (since k_0 , NA , U , and β are all λ -dependent). Taking the derivative of κ with respect to λ , it turns out that a larger diameter in the waist region ($\phi = 2r_0$) leads to a smaller $|d\kappa/d\lambda|$. Thus, for similar fibers and equal fusion lengths (L), a coupler with a larger ϕ is less wavelength-dependent and could be optimized for broadband applications [7].

III. NUMERICAL SIMULATIONS

Here we numerically investigate the effect of the waist section diameter and stretching level during the fabrication of an As_2Se_3 coupler on its fundamental features: coupling length and transmission spectrum. We assume that the two fibers remain in contact with each other during the fabrication process and no extra interdiffusion occurs when tapering them. CMT is used for numerical analysis in order to calculate κ in equation (1-b). The propagation constant (β) is obtained by solving the characteristic equation for an infinite-cladding cylindrical waveguide to obtain the electric field distribution (\vec{E}) and the magnetic field distribution (\vec{H}) of the fundamental mode. At any extension value, the diameter of each fiber is known from the heat-brush method which is fully described in [8].

Figure 1 illustrates the geometry of an As_2Se_3 coupler. Light is launched at the input port and adiabatically propagates along the transition region (TrR) and then reaches the waist region (WR), where the fibers are fused together and coupling occurs between them. The optical power present in each fiber adiabatically transforms back to the fundamental mode of the corresponding fiber [9] and is measured at the through and cross output ports.

Figure 2 illustrates the calculated coupling length as a function of the tapering extension. The more the two fibers are stretched, the deeper they fuse into each other, and a stronger coupling occurs between them (larger κ); as a result, the coupling length (L_c) decreases.

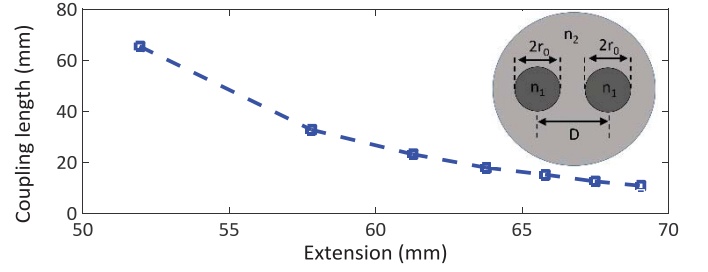


Fig. 2. Coupling length versus extension, calculated using CMT. The inset depicts the cross-section geometry of the coupler in the waist region.

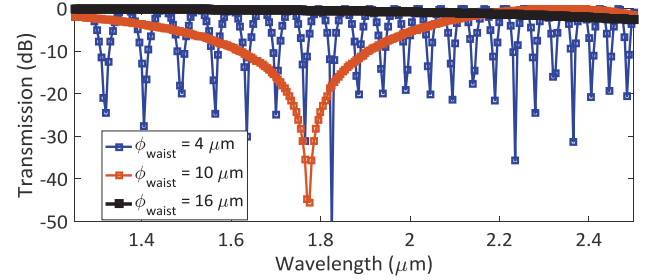


Fig. 3. Comparison between ChG couplers transmission spectra with different waist region diameters (ϕ). The black and blue traces correspond to broadband and wavelength-dependent couplers, respectively.

In order to investigate the effect of variable waist section diameter on the transmission spectrum, three couplers are studied numerically with different ϕ s. A fusion length of 4 cm is assumed for all three couplers. Figure 3 demonstrates the transmission spectra of ChG couplers with $\phi = 4\mu\text{m}$, $\phi = 10\mu\text{m}$ and $\phi = 16\mu\text{m}$. From this figure, the smaller the ϕ is, the more wavelength-selective the coupler will be. This is expected from theory since as the fibers are stretched, the diameter in the waist region is reduced; thus, the fundamental mode of each fiber expands and overlaps more with the other fiber; this leads to a larger κ which corresponds to an increased wavelength-dependence of the transmission spectrum (equation 2). ChG couplers with waist diameters of $4\mu\text{m}$ and $16\mu\text{m}$ correspond to the wavelength-dependent and broadband couplers presented in this letter, respectively.

IV. FABRICATION

The fibers used for the fabrication of As_2Se_3 couplers have initial core diameters of $7.0\mu\text{m}$ and $14.0\mu\text{m}$, targeting broadband and wavelength-dependent functionalities, respectively. The core and cladding materials are both As_2Se_3 glass with a slight variation of stoichiometry, resulting in a numerical aperture of $NA = 0.184$. In order to get quasi single-mode broadband coupling, the pair of fibers must be initially single-mode with $V < 2.405$. Several techniques have been proposed to fabricate fused optical couplers [8], [10]–[12] among which the heat-brush technique is known to be robust and guarantees the adiabaticity criteria as well [8]. Figure 4 shows a schematic of the heat-brush tapering setup used to pretaper the fibers as well as to make the couplers from pairs of juxtaposed fibers. For the pretapering stage, fibers are individually stretched to a predetermined uniform diameter. The ChG fiber ends are then polished, butt-coupled to silica fibers (SMF-28) and bonded

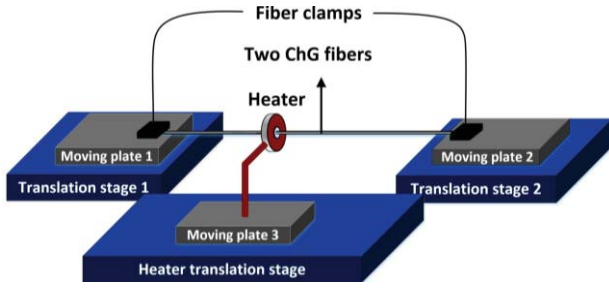


Fig. 4. Schematic of the tapering setup.

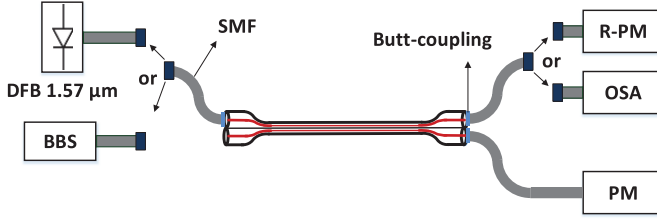


Fig. 5. Schematic of a coupler in the measurement setup. BBS, Broadband source; DFB, distributed feedback laser; PM, power meter; OSA, optical spectrum analyzer.

permanently using UV epoxy. The SMF-to-SMF insertion loss for the resulting $5.5 \mu\text{m}$ and $12.0 \mu\text{m}$ core pretapered fibers is $\sim 3 \text{ dB}$ and $\sim 5 \text{ dB}$ respectively, caused by the fundamental mode mismatch between the SMF and ChG fibers, Fresnel reflection losses, and misalignment between ChG fibers and SMF-28. The fibers with core diameters of $5.5 \mu\text{m}$ are single-mode with $V=2.05$ while the fibers with core diameters of $12.0 \mu\text{m}$ are multimode with $V=4.46$.

Symmetric fiber pairs are laid in the tapering setup for the coupler fabrication. A twist of one-half of a turn is performed on the fiber pair in order to keep them in contact during the tapering process. The heater temperature is set to $\sim 190^\circ\text{C}$, within the range of temperatures for which As_2Se_3 glass softens without collapsing. This optimal temperature allows the two fibers to be tapered and fused successfully while avoiding any undesirable interdiffusion between core and cladding materials, or a sudden breaking of the taper.

Figure 5 shows a schematic of the setup used for coupler characterization. A DFB laser (ANDO AQ4321A) emitting at a wavelength of $1.57 \mu\text{m}$ with 0 dBm output power is connected to the input port of the coupler. The output powers from the through and cross ports are measured *in situ* during the tapering process using power meters (PM). Periodically during the stretching process, the DFB laser and PM-through port are replaced with a broadband source (BBS, NKT SuperK COMPACT) and an optical spectrum analyzer (OSA) to measure the transmission spectrum of the through port. The BBS is set to have an output power of 0 dBm .

V. CHARACTERIZATION OF COUPLERS

Figure 6 shows the through port output power as a function of fiber extension for a typical coupler composed of two ChG fibers with initial core and cladding diameters of $5.5 \mu\text{m}$ and $136 \mu\text{m}$, respectively. The final cladding waist diameter and fusion length of the coupler are set

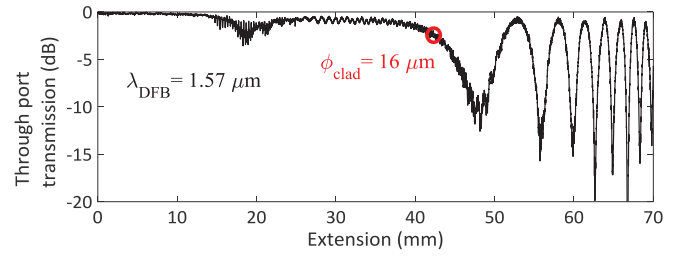


Fig. 6. Through port transmission as a function of extension. Annotation corresponds to a 50%-50% quasi single-mode coupler.

to $4 \mu\text{m}$ and 4 cm , respectively. Choosing these extreme values allows to fully observe the evolution of the coupling process as seen in Fig. 6. A complete transfer of power to the cross-port occurs at an extension length of 49 mm , and at this point, the coupler length equals L_c . Further extension of the coupler leads to multiple power transfers between the two fiber cores. The action of tapering slightly increases the losses with respect to un-tapered fibers. This excess loss is measured to be only 0.4 dB , leading to a total insertion loss from SMF to SMF input/output of 3.4 dB for this coupler.

It is interpreted from Fig. 6 that the fabricated coupler preserves well its symmetry. Considering a maximum power exchange of 20 dB between the ports in Fig. 6, one can use CMT to calculate the phase mismatch parameter in terms of κ for this coupler:

$$\delta = \frac{1}{10} |\kappa| \quad (4)$$

which is considered an extremely low phase mismatch and corresponding to an excellent symmetry of the coupler geometry. As equations (1-a) and (1-c) suggest, such an excellent symmetry enables the realization of couplers with coupling ratios as low as 1%-99% (or 20 dB).

The fabrication of a broadband 50%-50% coupler involves interrupting the extension at $\sim 43.2 \text{ mm}$ which is annotated in Fig. 6. In this case, a weak coupling is desired not to induce any wavelength-dependent coupling. In addition, the fusion length has to be chosen in the neighborhood of L_c depending on the target coupling ratio. This allows for only a few power cycles to be established between the two ports which is a requirement in a broadband coupler. To this end, the cladding diameter is reduced from the initial value of $136 \mu\text{m}$ to $16.0 \mu\text{m}$ in the waist region. The fusion length is set to only 1.18 cm . At this point, the core diameter is reduced from the initial value of $5.5 \mu\text{m}$ to $\sim 1 \mu\text{m}$ which satisfies the single-mode condition ($V < 2.405$); however, the propagating mode expands enough to interact with the ChG-Air boundary. Choosing a short fusion length not only provides a weak coupling which is required for the broadband operation, but it also avoids the excitation of higher order modes in the resulting three-layer ChG-ChG-Air waveguide due to surface roughness coupling. Figure 7(a) illustrates the normalized transmission spectra of a broadband coupler which provides a 50%-50% splitting ratio at $1.57 \mu\text{m}$. The transmission remains relatively close to 3 dB over a wavelength span of 500 nm , without any large and cyclic power variations observed in wavelength-dependent couplers. This highlights the fact that

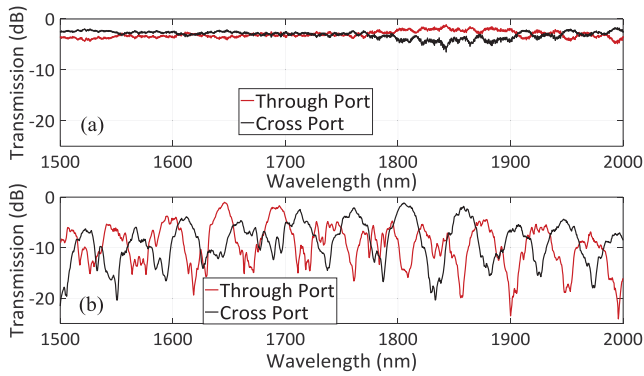


Fig. 7. Transmission spectra of (a) broadband and (b) wavelength-dependent ChG couplers.

this coupler has a length comparable to one-half the coupling length at a wavelength of $1.57 \mu\text{m}$. This broadband coupler is also quasi single-mode. This is verified from the lack of modal interference in its transmission spectra.

The fabrication recipe for a wavelength-dependent coupler differs from the broadband one, by the waist region diameter and fusion length. A pair of As_2Se_3 fibers with initial core and cladding diameters of $12.0 \mu\text{m}$ and $136 \mu\text{m}$, respectively, are adiabatically stretched down to a cladding waist diameter of $6.8 \mu\text{m}$. At this small diameter, the core completely vanishes ($<0.6 \mu\text{m}$) and the light is guided by the resulting ChG-Air waveguide with $V = 36.5$. At this fusion level, the coupling coefficient is large enough to induce a wavelength-dependent coupling in the wavelength range of $1.5\text{--}2.0 \mu\text{m}$. In addition, the fusion length is set at 4 cm , which corresponds to $\sim 25L_c$ and allows ~ 12.5 coupling cycles in between the two ports. Figure 7(b) depicts the normalized transmission spectrum of this coupler. An extinction ratio up to 15 dB is achieved between the through and cross ports. A periodicity of $\sim 6.25 \text{ THz}$ ($\sim 50 \text{ nm}$ at a wavelength of $1.55 \mu\text{m}$) is measured in the frequency domain. The periodicity of the wavelength-dependent coupler can be easily tuned with an appropriate ratio in between the fusion length and the coupling length. This is achievable since the transmission spectrum is readily measured *in situ* during the stretching process. The motion controller could be manually stopped as soon as a desired periodicity is observed on the OSA. The noisy oscillations of the wavelength-dependent spectrum are attributed to the modal interference in the multimode fusion length.

Take note that for both broadband and wavelength-dependent couplers, the transmission spectra are independent of the input state of polarization, as observed by placing a linear polarizer and a polarization controller after the BBS.

The transmission spectra of typical broadband and wavelength-dependent As_2Se_3 couplers are investigated, next. Figure 8(a) and (b) present the transmission spectra of As_2Se_3 couplers in the wavelength range of $\lambda = 4 \mu\text{m}$ and $\lambda = 10.5 \mu\text{m}$ to exemplify the applications of couplers compatible with holmium-doped fibers or CO_2 gas lasers. The fusion length is chosen to be 4 cm in all cases. The results confirm that by selecting proper waist diameters and fusion lengths,

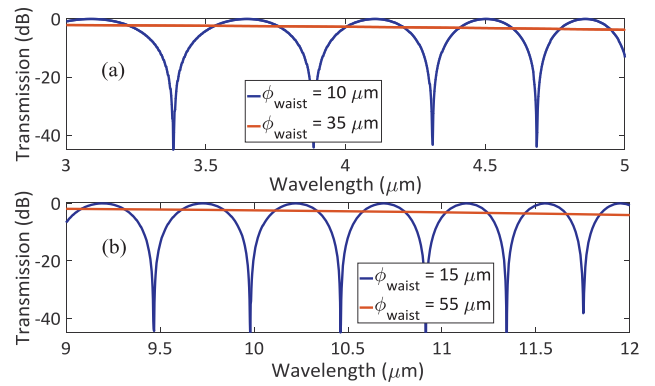


Fig. 8. Transmission spectra of broadband and wavelength-dependent As_2Se_3 couplers in the wavelength range of (a) $\lambda = 4 \mu\text{m}$ and (b) $\lambda = 10.5 \mu\text{m}$.

broadband and wavelength-dependent ChG couplers could be successfully designed at target mid-infrared bands.

VI. CONCLUSION

We introduced two ChG optical couplers based on As_2Se_3 fibers; one is a quasi-single-mode broadband coupler and the other is wavelength-dependent. The influence of extension length and waist diameter on coupler characteristics was studied numerically using CMT. The fabricated couplers are highly symmetric leading to variable coupling ratios ranging from 50%-50% down to 1%-99% at the through-cross ports. Thanks to the wide transparency window of As_2Se_3 glass, scaled versions of these couplers are expected to cover the $2\text{--}12 \mu\text{m}$ wavelengths of the mid-infrared.

REFERENCES

- [1] I. D. Aggarwal and J. S. Sanghera, "Development and applications of chalcogenide glass optical fibers at NRL," *J. Optoelectron. Adv. Mater.*, vol. 4, no. 2, pp. 665–678, 2002.
- [2] D. T. Schaafsma, J. A. Moon, J. S. Sanghera, and I. D. Aggarwal, "Fused taper infrared optical fiber couplers in chalcogenide glass," *J. Lightw. Technol.*, vol. 15, no. 12, pp. 2242–2245, Dec. 1997.
- [3] D. T. Schaafsma and J. S. Sanghera, "Infrared optical fiber coupler," U.S. Patent 5949935 A, Sep. 7, 1999.
- [4] G. Stevens and T. Woodbridge, "Mid-IR fused fiber couplers," *Proc. SPIE*, vol. 9730, p. 973007, Apr. 2016.
- [5] R. R. Gattass, R. Thapa, F. H. Kung, L. E. Busse, L. B. Shaw, and J. S. Sanghera, "Review of infrared fiber-based components," *Appl. Opt.*, vol. 54, no. 31, pp. F25–F34, 2015.
- [6] J. M. Liu, *Photonic Devices*. Cambridge, U.K.: Cambridge Univ. Press, 2005, ch. 4.
- [7] J. Bures, S. Lacroix, and J. Lapierre, "Analyse d'un coupleur bidirectionnel à fibres optiques monomodes fusionnées," *Appl. Opt.*, vol. 22, no. 12, pp. 1918–1922, 1983.
- [8] C. Baker and M. Rochette, "A generalized heat-brush approach for precise control of the waist profile in fiber tapers," *Opt. Mater. Exp.*, vol. 1, no. 6, pp. 1065–1076, 2011.
- [9] J. D. Love, W. M. Henry, W. J. Stewart, R. J. Black, S. Lacroix, and F. Gonthier, "Tapered single-mode fibres and devices. Part 1: Adiabaticity criteria," *IEE Proc. J-Optoelectron.*, vol. 138, no. 5, pp. 343–354, Oct. 1991.
- [10] G. Georgiou and A. C. Boucouvalas, "Low-loss single-mode optical couplers," *IEE Proc. J-Optoelectron.*, vol. 132, no. 5, pp. 297–302, Oct. 1985.
- [11] D. B. Mortimore, "Theory and fabrication of 4×4 single-mode fused optical fiber couplers," *Appl. Opt.*, vol. 29, no. 3, pp. 371–374, 1990.
- [12] F. Bilodeau, K. O. Hill, D. C. Johnson, and S. Faucher, "Compact, low-loss, fused biconical taper couplers: Overcoupled operation and antisymmetric supermode cutoff," *Opt. Lett.*, vol. 12, no. 8, pp. 634–636, 1987.